Mechanical Engineering Publications   Mechanical Engineering

1-1-2007

Orthogonal Linear Regression in Roentgen Stereophotogrammetry

Patrick Atkinson
Kettering University, patkinso@kettering.edu

Jesse V. Benny

Brian J. McCartin

Recommended Citation

Orthogonal Linear Regression in Roentgen Stereophotogrammetry

Jesse V. Benny, Brian J. M$^{\underline{c}}$Cartin[1], Patrick J. Atkinson

Kettering University
1700 West Third Avenue, Flint, MI 48504-4898 USA

Abstract

Rooted in aerial reconnaissance, mathematical photogrammetry has evolved into a mainstay of biomedical image processing. The present paper develops an algorithm for Roentgen stereophotogrammetry, a method of imaging musculoskeletal systems both static and dynamic, which incorporates a number of novel features employing techniques from projective geometry, orthogonal regression and least squares approximation. Theoretical and numerical evidence is presented of the efficacy of the proposed procedure.

1   Introduction

Mathematical photogrammetry is an amalgam of projective geometry and statistical analysis [1] which extracts spatial and spatio-temporal information from two dimensional images produced by electromagnetic or acoustical radiation. Originally developed in the context of aerial photography applied to the compilation of topographic maps and surveys [2], it has emerged as a principal analytical tool in the biomedical sciences [3].

When a pair of photographs (i.e., a stereoscopic pair) taken from different perspective views is employed, this technique is called stereophotogrammetry. When x-rays are substituted for the photographs, this mode of analysis is called Roentgen Stereophotogrammetric Analysis (RSA) [4, 5]. RSA has been used extensively in recent years to study the biomechanics and kinematics of musculoskeletal systems [6].

---

[1]Corresponding author. Email: bmccarti@kettering.edu
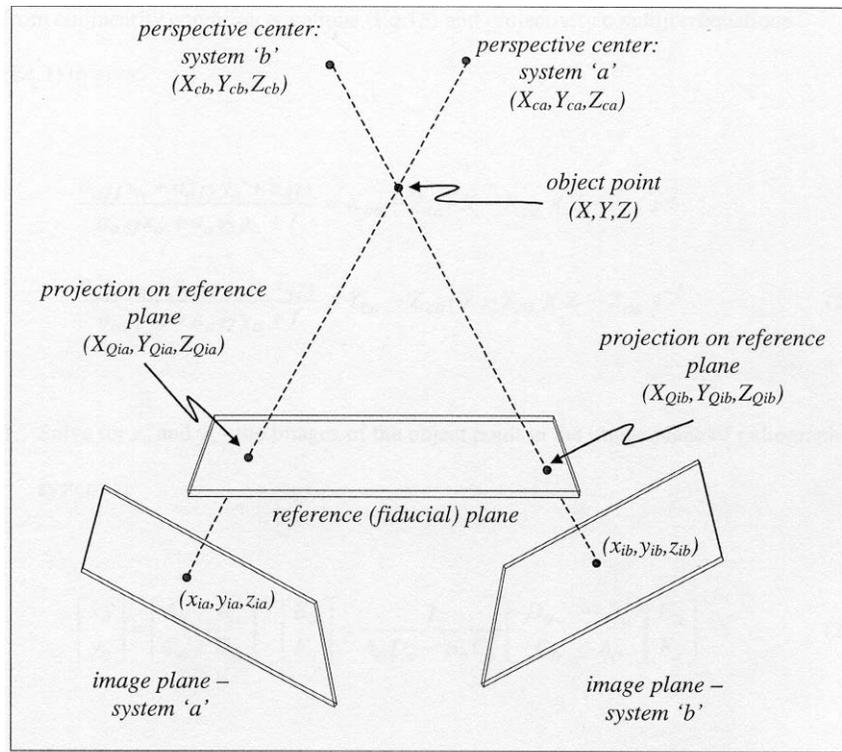
Figure 1: Schematic for Roentgen Stereophotogrammetric Analysis

These RSA musculoskeletal studies include cranio-facial analysis; the study of the movements of the hand, knee, ankle/foot complex, shoulder joint and pelvic joints as well as the shape of the spine; and to the detection of loosening in total joint replacements of the hip and knee.

Despite these triumphs, RSA is an error prone procedure with inaccuracies arising from image parallax, operator measurement error, x-ray film unflatness, undulations on the reference plane of the calibration device, and errors in the measured reference marker positions. The present paper presents some novel ways to reduce these myriad errors.

In what follows, we first present the formulation of the basic mathematical problem of RSA. We then present a complete algorithm for the solution of this problem with emphasis on the unique features of our approach. Next, we present experimental evidence of the efficacy of this algorithm. Finally, we draw some general conclusions and discuss ways in which our algorithm has been applied in practice.

2 RSA Problem Formulation
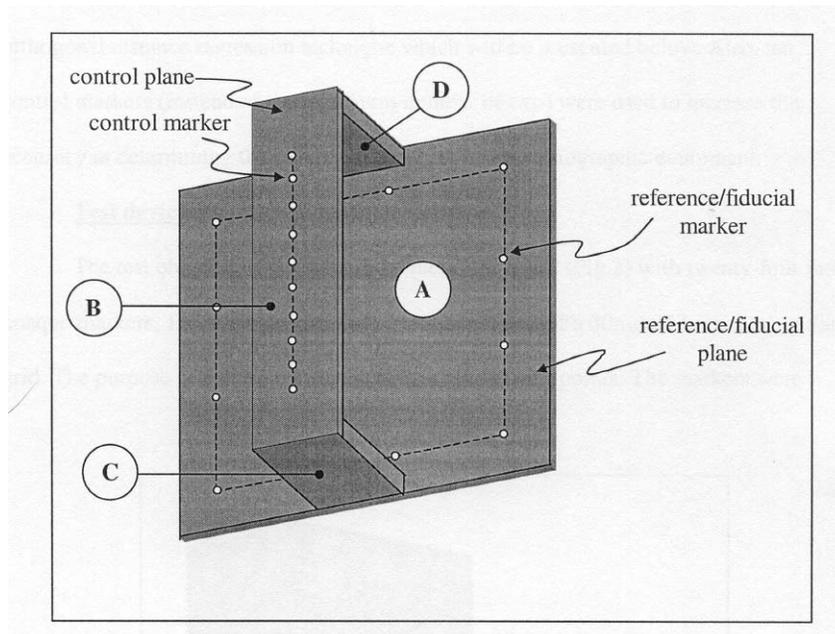
Figure 2: Calibration Device

With reference to Figure 1, the basic principle underlying Roentgen Stereophotogrammetric Analysis (RSA) is the noninvasive, nondestructive acquisition of three-dimensional coordinates of skeletal landmark (object) points in the relevant anatomy. This is achieved by first acquiring two-dimensional measurements of stereoradiographic images of radio-opaque markers implanted in the specimen, followed by a mathematical reconstruction of their actual spatial positions with respect to a laboratory coordinate system attached to the reference (fiducial) plane.

The mathematical reconstruction procedure requires that the radiographic systems first be calibrated. For this purpose, a calibration device (Figure 2) having two sets of easily identifiable radio-opaque markers (fiducial/reference points and control points) is employed. The three-dimensional coordinates of the fiducial and control points are determined *a priori* relative to the laboratory coordinate system which contains the plane of the fiducial points as one of its coordinate planes.

As such, this methodology is prone to errors arising from image parallax, operator measurement error, x-ray film unflatness, deviations from ideal flatness of the fiducial plane of the calibration device, and errors in the *a priori* measured fiducial and control marker positions. The RSA algorithm proper
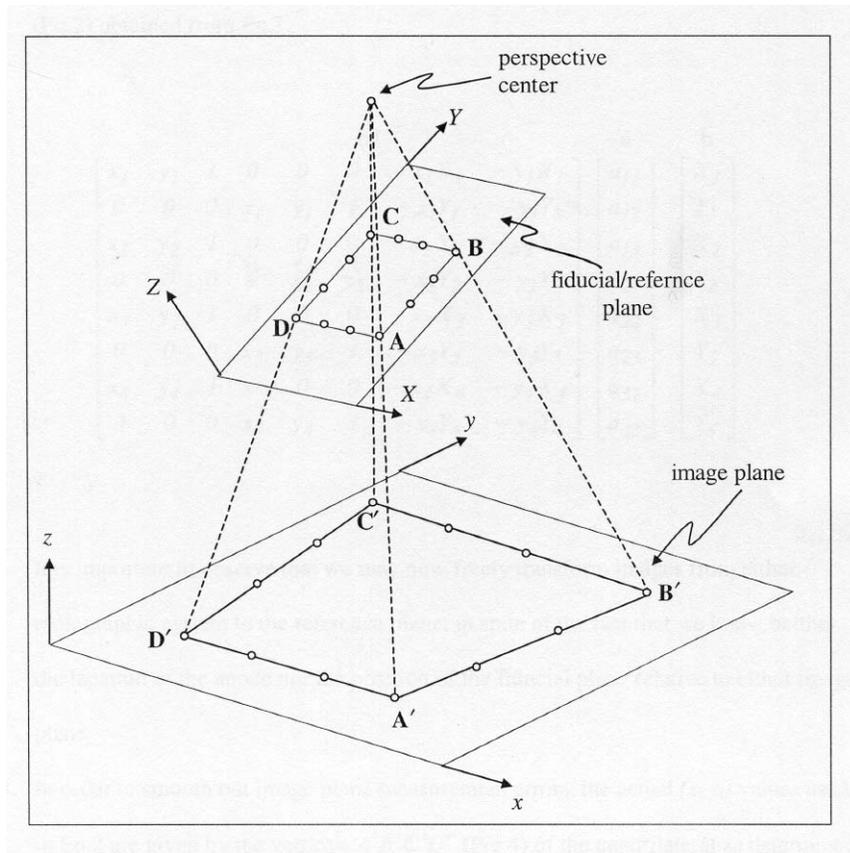
Figure 3: Projective Transformation

may be partitioned into three phases each with its own sources of error: determination of the perspective relations, prediction of the perspective center (anode) locations, and the estimation of the experimental marker positions.

Firstly, the perspective transformations which serve to relate the reference and image plane coordinates may be determined without *a priori* knowledge of the location of the perspective center [7] (Figure 3). Thus, the determination of the perspective relations is prone to two sources of error: the determination of the reference point marker coordinates relative to the local reference plane coordinate system and the error associated with the measurement of the location of the images of these points on the image planes. Below, we propose a linear orthogonal distance regression (LODR) procedure [8] to simultaneously address both sources of error (Figure 4).

Secondly, the prediction of the location of the anode centers is prone to three sources of error: the diffuse location of the anode sources (i.e. they are not ideal points), operator errors in the measurement of the control point images on the image planes, and errors in the three-dimensional spatial coor-
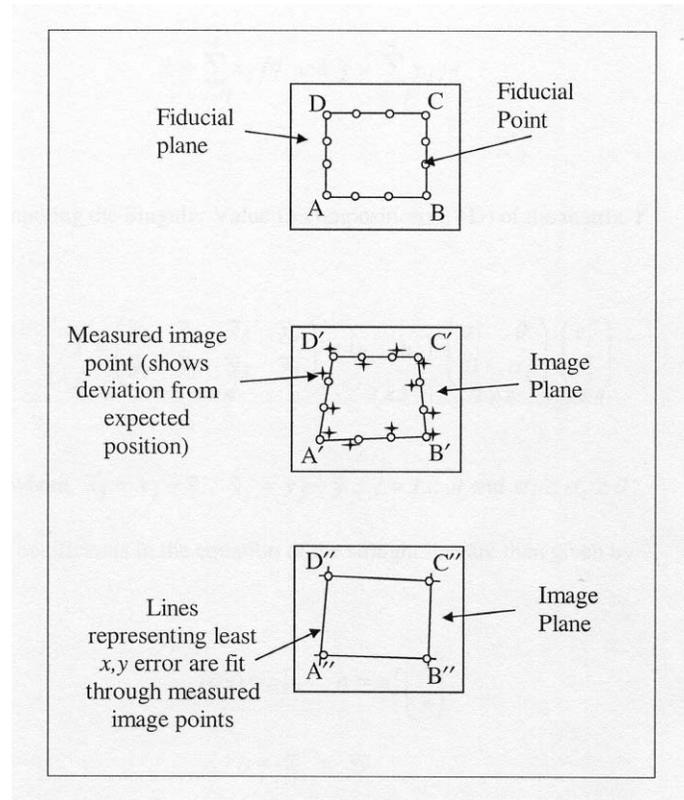
Figure 4: Linear Orthogonal Distance Regression

dinates of the control points. The first two sources of error are treated via least squares adjustments of the collinearity equations directly on the image planes where they actually occur (see Figure 5). Traditionally, these adjustments have been made on the reference plane which requires estimates of the error variances in the spatial coordinates of the reference system. The third source of error is treated by a combined parametric-condition adjustment [5].

Thirdly, the estimation of the three-dimensional coordinates of the experimental markers is based upon a spatial intersection of the two independent radiographic systems. Once again, the diffuse location of the anode focal points and the operator measurement of object point images are potential sources of error. As above, these errors are treated by least squares adjustment directly on the image planes rather than prior transformation to the reference plane.

We now turn to the development of an algorithm for the solution of this RSA problem. While hybridizing the best of algorithms of Selvik [4] and Veress [5], our algorithm incorporates a number of novel features. Linear orthogonal distance regression (LODR) is employed to minimize the error made during the measurements of the two-dimensional image locations of the fiducial markers
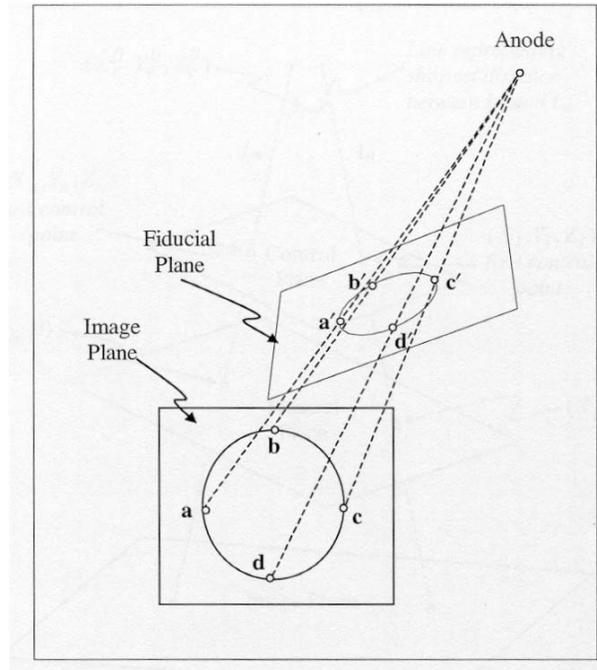
Figure 5: Introduction of Biased Errors

of the calibration device. An improved least squares procedure based upon the collinearity equations with adjustments on the image planes and accounting for control point errors is utilized to provide more accurate predictions of perspective center (anode) locations of the radiographic systems. Likewise, this improved least squares procedure using image plane adjustments also provides enhanced accuracy in predicting the actual spatial positions of the markers implanted in the specimen.

3   RSA Algorithm Development

The description of our RSA algorithm will be subdivided into three parts. The first two parts concern the calibration of the radiographic systems. These are the determination of the perspective relations by LODR and the prediction of the locations of the perspective centers by a least squares solution of the collinearity equations. The third part involves the estimation of the three-dimensional coordinates of the object points by a least squares space intersection procedure.
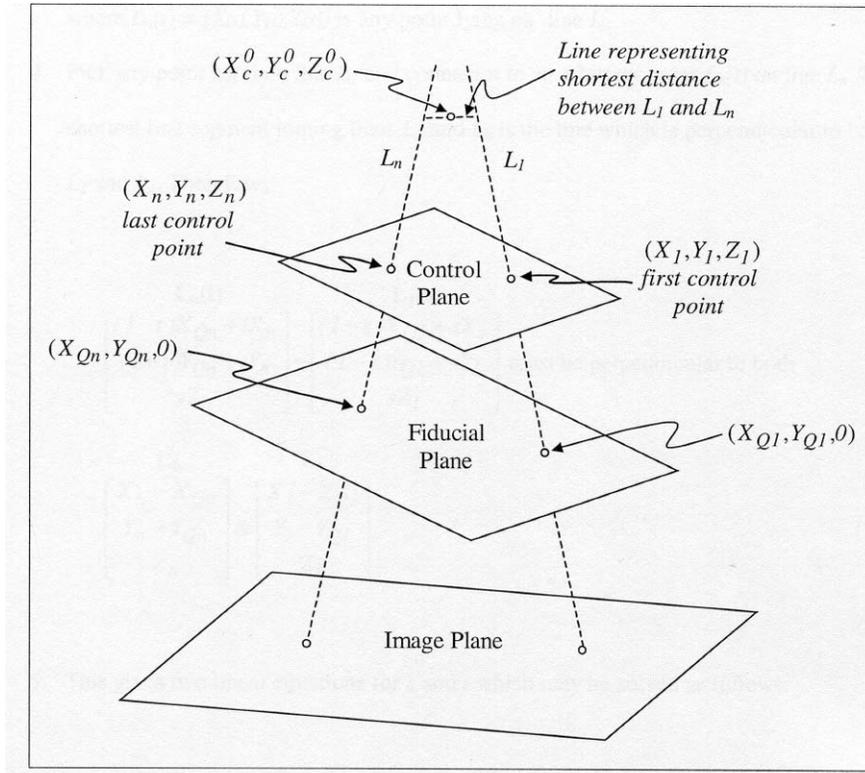
Figure 6: Estimation of Perspective Center Location

3.1 Determination of Perspective Relations by LODR

With reference to Figure 3, we must establish a mathematical relationship between the fiducial plane and the image plane for each of the two radiographic systems. To achieve this, we will avail ourselves of the following foundational result due to Möbius [**7, p. 105**]:

Theorem 1 (The Fundamental Theorem of Projective Geometry)
There exists a unique two-dimensional projective transformation of the points of a plane M' into the points of a plane M which carries four given points, no three collinear, in M' respectively into four prescribed points, no three collinear, in M.

The projective tranformation whose existence is guaranteed by this theorem may be explicitly constructed as

$$X = f(x, y) = \frac{a_{11}x + a_{12}y + a_{13}}{a_{31}x + a_{32}y + 1}; \ Y = g(x, y) = \frac{a_{21}x + a_{22}y + a_{23}}{a_{31}x + a_{32}y + 1}, \quad (1)$$

where the transformation coefficients are obtained by solving the system of

linear equations

$$
\begin{bmatrix}
x_1 & y_1 & 1 & 0 & 0 & 0 & -x_1X_1 & -y_1X_1 \\
0 & 0 & 0 & x_1 & y_1 & 1 & -x_1Y_1 & -y_1Y_1 \\
x_2 & y_2 & 1 & 0 & 0 & 0 & -x_2X_2 & -y_2X_2 \\
0 & 0 & 0 & x_2 & y_2 & 1 & -x_2Y_2 & -y_2Y_2 \\
x_3 & y_3 & 1 & 0 & 0 & 0 & -x_3X_3 & -y_3X_3 \\
0 & 0 & 0 & x_3 & y_3 & 1 & -x_3Y_3 & -y_3Y_3 \\
x_4 & y_4 & 1 & 0 & 0 & 0 & -x_4X_4 & -y_4X_4 \\
0 & 0 & 0 & x_4 & y_4 & 1 & -x_4Y_4 & -y_4Y_4
\end{bmatrix}
\begin{bmatrix}
a_{11} \\ a_{12} \\ a_{13} \\ a_{21} \\ a_{22} \\ a_{23} \\ a_{31} \\ a_{32}
\end{bmatrix}
=
\begin{bmatrix}
X_1 \\ Y_1 \\ X_2 \\ Y_2 \\ X_3 \\ Y_3 \\ X_4 \\ Y_4
\end{bmatrix}.
\tag{2}
$$

As illustrated in Figure 3, the (x, y, z) coordinate systems are attached to the image planes while the (X, Y, Z) coordinate system is attached to the fiducial/reference plane. The coordinates (x_i, y_i) and (X_i, Y_i) for $i = 1, 2, 3, 4$ which appear in Equation (2) are those of the corresponding points referred to in Theorem 1 which appear as A', B', C', D' and A, B, C, D, respectively, in Figure 3.

If these coordinates were known exactly then Equation (2) would provide an entirely satisfactory means of determining the coefficients of the projective transformation, Equation (1). However, as these are in fact measured quantities, they are tainted with error. As this projective transformation is the cornerstone of the remaining stages of our RSA algorithm, it is of paramount importance that these errors be suppressed.

We provide such numerical smoothing by introducing additional fiducial points along the periphery of the rectangle $ABCD$ of Figure 3. Specifically, we employ four equally spaced points $(\hat{X}_i, \hat{Y}_i)$; $i = 1, 2, 3, 4$ along each edge of the rectangle for a total of twelve fiducial markers. The corresponding measured image coordinates are denoted by $(\hat{x}_i, \hat{y}_i)$; $i = 1, 2, 3, 4$.

As is evident from Figure 4, the error present in these measured image coordinates makes it impossible to determine the exact image quadrilateral $A'B'C'D'$. Thus, we resort to linear orthogonal distance regression (LODR) [8, pp. 184-186] to fit each side of the image quadrilateral. The fitted image quadrilateral $A''B''C''D''$ is then obtained from the intersection of these four lines. The details are as follows.

Along each edge, we seek the straight line defined by

$$
cx + sy = h; \ c^2 + s^2 = 1
\tag{3}
$$

which minimizes the sum of squares of the orthogonal distances from the data points. Defining the mean coordinates as

$$
\bar{x} = \frac{1}{4} \sum_{i=1}^{4} \hat{x}_i; \ \bar{y} = \frac{1}{4} \sum_{i=1}^{4} \hat{y}_i,
\tag{4}
$$

we compute the Singular Value Decomposition (SVD) of the shifted data matrix

$$M = \begin{bmatrix} \hat{x}_1 - \bar{x} & \hat{x}_2 - \bar{x} & \hat{x}_3 - \bar{x} & \hat{x}_4 - \bar{x} \\ \hat{y}_1 - \bar{y} & \hat{y}_2 - \bar{y} & \hat{y}_3 - \bar{y} & \hat{y}_4 - \bar{y} \end{bmatrix} = \begin{bmatrix} u_1 & u_2 \end{bmatrix} \begin{bmatrix} \sigma_1 & 0 \\ 0 & \sigma_2 \end{bmatrix} \begin{bmatrix} v_1^T \\ v_2^T \end{bmatrix},$$
(5)

where $\sigma_1 \geq \sigma_2 \geq 0$. The orthogonal regression coefficients are then given by

$$[c \; s] = u_2^T; \;\; h = c\bar{x} + s\bar{y}.$$
(6)

Performing this SVD process along each edge of the quadrilateral, the intersection of consecutive edges provides the vertices of the LODR-fitted quadrilateral $A''B''C''D''$ of Figure 4. The coordinates of these vertices are then used in Equation (2) to determine the coefficients of the perspective relations, Equation (1). It is straightforward to extend this technique to an arbitrary number of fiducial markers.

The use of orthogonal regression presumes that errors in the two coordinate directions are uncorrelated and of equal variance. If the variances are not equal then λ-regression may be employed [9] while if the errors are correlated then (λ, μ)-regression may be employed [10]. It is important to observe that, with the aid of Equation (1), we may now freely transform images from either radiographic system to the reference plane, in spite of the fact that we know neither the locations of the perspective centers (anodes) nor the position of the fiducial plane relative to either image plane!

3.2   Location of Perspective Centers by Collinearity

The calibration process not only involves the determination of the perspective relations as described above but also the prediction of the perspective center (anode) locations. These are denoted by (X_{ca}, Y_{ca}, Z_{ca}) and (X_{cb}, Y_{cb}, Z_{cb}) in Figure 1. For this purpose, we utilize the control markers shown in Figure 2.

We base our initial estimate of the location of each perspective center upon the midpoint of the shortest line segment joining the rays passing through the two control points furthest from one another (Figure 6). This can be achieved in an explicit non-iterative fashion. We then improve upon this estimate via an iterative least squares solution of the collinearity equations, to be derived below, for all of the control points (Figure 7).

Least squares adjustment to account for all sources of error (including measurement errors in the control point coordinates themselves) takes place directly on the image planes. As is evident from Figure 5, this avoids the introduction of biased errors which would occur if the adjustments were instead made on the fiducial plane. We thereby avoid the unnecessary complication of estimating the error variances of weighted least squares.
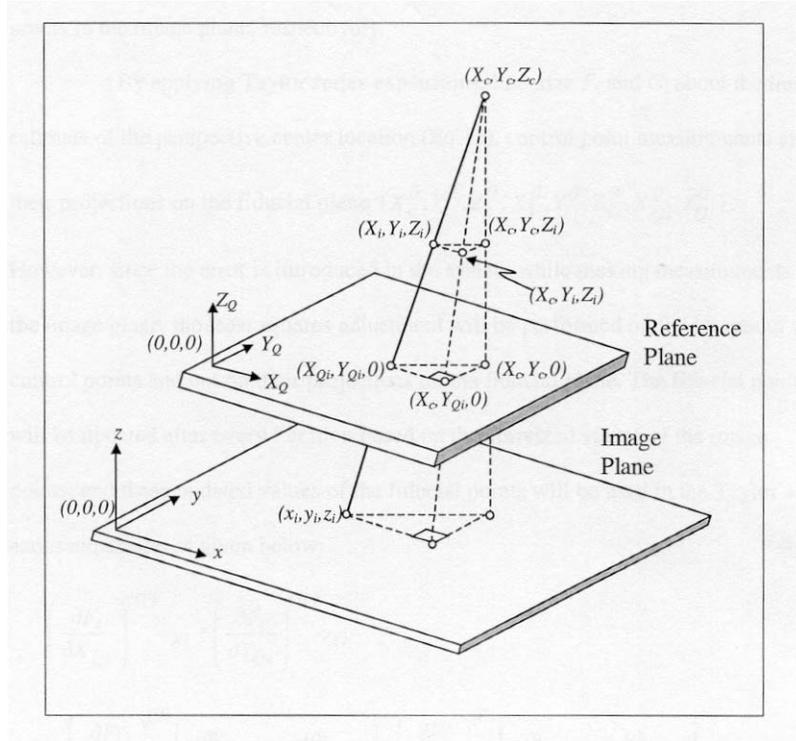
Figure 7: Coordinate Systems for Collinearity Equations

3.2.1   Initial Guess

With reference to Figure 6, consider the two control points furthest from one another, (X_1, Y_1, Z_1) and (X_n, Y_n, Z_n), together with their projections onto the fiducial plane, $(X_{Q1}, Y_{Q1}, Z_{Q1} = 0)$ and $(X_{Qn}, Y_{Qn}, Z_{Qn} = 0)$, respectively. Now, fit a straight line through each of these pairs of corresponding points in parametric form:

$$L_1 : \ X(s) = (1-s)X_{Q1} + sX_1, \ Y(s) = (1-s)Y_{Q1} + sY_1, Z(s) = sZ_1, \quad (7)$$

and

$$L_n : \ X(t) = (1-t)X_{Qn} + tX_n, \ Y(t) = (1-t)Y_{Qn} + tY_n, Z(t) = tZ_n. \quad (8)$$

The shortest line segment connecting these two lines must be perpendicular to each line. Thus,

$$\begin{bmatrix} (1-t)X_{Qn} + tX_n - (1-s)X_{Q1} - sX_1 \\ (1-t)Y_{Qn} + tY_n - (1-s)Y_{Q1} - sY_1 \\ tZ_n - sZ_1 \end{bmatrix} \perp \begin{bmatrix} X_1 - X_{Q1} \\ Y_1 - Y_{Q1} \\ Z_1 \end{bmatrix} \& \begin{bmatrix} X_n - X_{Qn} \\ Y_n - Y_{Qn} \\ Z_n \end{bmatrix}.$$
$$(9)$$

These orthogonality conditions provide two linear equations for the determination of s and t:

$$\begin{bmatrix} A_{11} & A_{12} \\ A_{21} & A_{22} \end{bmatrix} \begin{bmatrix} s \\ t \end{bmatrix} = \begin{bmatrix} B_1 \\ B_2 \end{bmatrix}, \tag{10}$$

where

$$A_{11} = (X_1 - X_{Q1})^2 + (Y_1 - Y_{Q1})^2 + Z_1^2,$$

$$A_{12} = A_{21} = -(X_n - X_{Qn})(X_1 - X_{Q1}) - (Y_n - Y_{Qn})(Y_1 - Y_{Q1}) - Z_1 Z_n,$$

$$A_{22} = (X_n - X_{Qn})^2 + (Y_n - Y_{Qn})^2 + Z_n^2,$$

$$B_1 = (X_{Qn} - X_{Q1})(X_1 - X_{Q1}) + (Y_{Qn} - Y_{Q1})(Y_1 - Y_{Q1}),$$

$$B_2 = (X_{Q1} - X_{Qn})(X_n - X_{Qn}) + (Y_{Q1} - Y_{Qn})(Y_n - Y_{Qn}).$$

Our initial estimate of the location of each perspective center is now given by the midpoint of this shortest line segment connecting L_1 and L_n:

$$(X_c^0, Y_c^0, Z_c^0) = \frac{1}{2} \cdot \begin{bmatrix} (1-t)X_{Qn} + tX_n + (1-s)X_{Q1} + sX_1 \\ (1-t)Y_{Qn} + tY_n + (1-s)Y_{Q1} + sY_1 \\ tZ_n + sZ_1 \end{bmatrix}. \tag{11}$$

3.2.2 Iteration Procedure

The collinearity condition expresses the constraint that the perspective center, an object point, and its image all lie on a line. The collinearity equations expressing this condition follow from the similar triangles of Figure 7 as follows. For $i = 1, \ldots, n$,

$$\frac{X_{Qi} - X_c}{X_i - X_c} = \frac{Y_{Qi} - Y_c}{Y_i - Y_c} = \frac{Z_{Qi} - Z_c}{Z_i - Z_c}, \tag{12}$$

where n is the number of control points. Using $Z_{Qi} = 0$, Equation (12) may be rewritten as the pair of equations

$$\begin{aligned} F_i(X_c, Y_c, Z_c, X_i, Y_i, Z_i, X_{Qi}, Y_{Qi}) = \\ (X_{Qi} - X_c)(Z_i - Z_c) + Z_c(X_i - X_c) = 0, \\ G_i(X_c, Y_c, Z_c, X_i, Y_i, Z_i, X_{Qi}, Y_{Qi}) = \\ (Y_{Qi} - Y_c)(Z_i - Z_c) + Z_c(Y_i - Y_c) = 0. \end{aligned} \tag{13}$$

By virtue of the facts that X_c, Y_c, Z_c are unknown and the measured quantities $X_i, Y_i, Z_i, X_{Qi}, Y_{Qi}$ include error, we have $2n$ nonlinear equations in $5n+3$ unknowns. We will linearize these equations and then solve iteratively with linear least squares [2]. For the reason previously stated, the least squares adjustment to the control points will be performed on their projections onto the

image plane rather than their projections onto the fiducial plane. The fiducial points will be updated after each iteration based upon the updated values of the corresponding image points.

We will denote the initial guess at the anode location by (X_c^0, Y_c^0, Z_c^0) and the measured values of the control point coordinates and their projections by (X_i^0, Y_i^0, Z_i^0) and (x_{Qi}^0, y_{Qi}^0), respectively. Their respective least squares adjustments will be denoted by $(\Delta X_c, \Delta Y_c, \Delta Z_c)$, (u_{Xi}, u_{Yi}, u_{Zi}), and (v_{xi}, v_{yi}).

The linearized equations may be expressed as

$$D\vec{w} + A\vec{\Delta} = \vec{b}, \tag{14}$$

where the matrices are defined as follows:

$$A = \begin{bmatrix} \frac{\partial F_1}{\partial X_c} & \frac{\partial F_1}{\partial Y_c} & \frac{\partial F_1}{\partial Z_c} \\ \frac{\partial G_1}{\partial X_c} & \frac{\partial G_1}{\partial Y_c} & \frac{\partial G_1}{\partial Z_c} \\ \vdots & \vdots & \vdots \\ \frac{\partial F_n}{\partial X_c} & \frac{\partial F_n}{\partial Y_c} & \frac{\partial F_n}{\partial Z_c} \\ \frac{\partial G_n}{\partial X_c} & \frac{\partial G_n}{\partial Y_c} & \frac{\partial G_n}{\partial Z_c} \end{bmatrix}^{(0)} = \begin{bmatrix} -Z_1 & 0 & X_1 - X_{Q1} \\ 0 & -Z_1 & Y_1 - Y_{Q1} \\ \vdots & \vdots & \vdots \\ -Z_n & 0 & X_n - X_{Qn} \\ 0 & -Z_n & Y_n - Y_{Qn} \end{bmatrix}^{(0)}, \tag{15}$$

$$D = \mathrm{diag}(D_1, \ldots, D_n); \ D_i = \begin{bmatrix} \frac{\partial F_i}{\partial X_i} & \frac{\partial F_i}{\partial Y_i} & \frac{\partial F_i}{\partial Z_i} & \frac{\partial F_i}{\partial x_{Qi}} & \frac{\partial F_i}{\partial y_{Qi}} \\ \frac{\partial G_i}{\partial X_i} & \frac{\partial G_i}{\partial Y_i} & \frac{\partial G_i}{\partial Z_i} & \frac{\partial G_i}{\partial x_{Qi}} & \frac{\partial G_i}{\partial y_{Qi}} \end{bmatrix}^{(0)} =$$

$$\begin{bmatrix} Z_c & 0 & X_{Qi} - X_c & (Z_i - Z_c) \cdot f_x & (Z_i - Z_c) \cdot f_y \\ 0 & Z_c & Y_{Qi} - Y_c & (Z_i - Z_c) \cdot g_x & (Z_i - Z_c) \cdot g_y \end{bmatrix}^{(0)}, \tag{16}$$

$$\vec{b} = -[F_1^{(0)}, G_1^{(0)}, \ldots, F_n^{(0)}, G_n^{(0)}]^T; \ \vec{\Delta} = [\Delta X_c, \Delta Y_c, \Delta Z_c]^T, \tag{17}$$

$$\vec{w} = [u_{X1}, u_{Y1}, u_{Z1}, v_{x1}, v_{y1}, \ldots, u_{Xn}, u_{Yn}, u_{Zn}, v_{xn}, v_{yn}]^T, \tag{18}$$

with f and g as defined by Equation (1).

The linear least squares solution to Equation (14) is given by [2]

$$\vec{\Delta} = [A^T (DD^T)^{-1} A]^{-1} A^T (DD^T)^{-1} \vec{b}; \ \vec{w} = D^T (DD^T)^{-1} (\vec{b} - A\vec{\Delta}). \tag{19}$$

The values of (X_c^0, Y_c^0, Z_c^0), (X_i^0, Y_i^0, Z_i^0) and (x_{Qi}^0, y_{Qi}^0) may now be updated and the entire process repeated until convergence. In all cases investigated, our initial guess at the anode locations was sufficiently accurate to ensure convergence of the iteration.

3.3 Location of Object Points by Space Intersection

At the conclusion of the above steps, the calibration procedure is complete. Now that the perspective transformations have been determined relating the reference and image planes and the location of the perspective centers (anodes)

are known, the position of any object point in space may be determined by the space intersection procedure defined below.

With reference to Figure 1, the space intersection equations are derived from the collinearity equations, Equation (13), for each radiographic system and may be expressed as the full rank overdetermined system

$$A\vec{X} = \begin{bmatrix} Z_{ca} & 0 & X_{Qa} - X_{ca} \\ 0 & Z_{ca} & Y_{Qa} - Y_{ca} \\ Z_{cb} & 0 & X_{Qb} - X_{cb} \\ 0 & Z_{cb} & Y_{Qb} - Y_{cb} \end{bmatrix} \begin{bmatrix} X^0 \\ Y^0 \\ Z^0 \end{bmatrix} = \begin{bmatrix} X_{Qa} Z_{ca} \\ Y_{Qa} Z_{ca} \\ X_{Qb} Z_{cb} \\ Y_{Qb} Z_{cb} \end{bmatrix} = \vec{B}, \quad (20)$$

where the subscripts a and b refer to the two radiographic systems and (X^0, Y^0, Z^0) is the coordinate vector of the object point ignoring measurement errors. The linear least squares solution of Equation (20) is $\vec{X} = (A^T A)^{-1} A^T \vec{B}$. We will now perform an additional least squares adjustment to account for measurement errors.

First consider radiographic system a and equate the expressions for X_{Qa} and Y_{Qa} obtained from the projective transformation, Equation (1), and the collinearity condition, Equation (13). This yields

$$\frac{a_{11}^a x_a + a_{12}^a y_a + a_{13}^a}{a_{31}^a x_a + a_{32}^a y_a + 1} = X_{ca} - Z_{ca}(X - X_{ca})/(Z - Z_{ca}),$$
$$\frac{a_{21}^a x_a + a_{22}^a y_a + a_{23}^a}{a_{31}^a x_a + a_{32}^a y_a + 1} = Y_{ca} - Z_{ca}(Y - Y_{ca})/(Z - Z_{ca}). \quad (21)$$

Solving for x_a and y_a, we obtain

$$x_a = f_1(X, Y, Z) = \frac{D_a E_a - B_a F_a}{A_a D_a - B_a C_a},$$
$$y_a = f_2(X, Y, Z) = \frac{A_a F_a - C_a E_a}{A_a D_a - B_a C_a}, \quad (22)$$

where

$$\begin{aligned}
A_a &= a_{11}^a - a_{31}^a[X_{ca} - Z_{ca}(X - X_{ca})/(Z - Z_{ca})], \\
B_a &= a_{12}^a - a_{32}^a[X_{ca} - Z_{ca}(X - X_{ca})/(Z - Z_{ca})], \\
C_a &= a_{21}^a - a_{31}^a[Y_{ca} - Z_{ca}(Y - Y_{ca})/(Z - Z_{ca})], \\
D_a &= a_{22}^a - a_{32}^a[Y_{ca} - Z_{ca}(Y - Y_{ca})/(Z - Z_{ca})], \\
E_a &= [X_{ca} - Z_{ca}(X - X_{ca})/(Z - Z_{ca})] - a_{13}^a, \\
F_a &= [Y_{ca} - Z_{ca}(Y - Y_{ca})/(Z - Z_{ca})] - a_{23}^a.
\end{aligned}$$

Likewise, solving for x_b and y_b, we obtain

$$x_b = f_3(X, Y, Z) = \frac{D_b E_b - B_b F_b}{A_b D_b - B_b C_b},$$
$$y_b = f_4(X, Y, Z) = \frac{A_b F_b - C_b E_b}{A_b D_b - B_b C_b}, \quad (23)$$

where

$$
\begin{aligned}
A_b &= a_{11}^b - a_{31}^b[X_{cb} - Z_{cb}(X - X_{cb})/(Z - Z_{cb})], \\
B_b &= a_{12}^b - a_{32}^b[X_{cb} - Z_{cb}(X - X_{cb})/(Z - Z_{cb})], \\
C_b &= a_{21}^b - a_{31}^b[Y_{cb} - Z_{cb}(Y - Y_{cb})/(Z - Z_{cb})], \\
D_b &= a_{22}^b - a_{32}^b[Y_{cb} - Z_{cb}(Y - Y_{cb})/(Z - Z_{cb})], \\
E_b &= [X_{cb} - Z_{cb}(X - X_{cb})/(Z - Z_{cb})] - a_{13}^b, \\
F_b &= [Y_{cb} - Z_{cb}(Y - Y_{cb})/(Z - Z_{cb})] - a_{23}^b.
\end{aligned}
$$

We thus arrive at the residual vector

$$
\vec{u} = [u_1 \ u_2 \ u_3 \ u_4]^T = \vec{b} - J[\Delta X \ \Delta Y \ \Delta Z]^T, \tag{24}
$$

where

$$
\vec{b} = \begin{bmatrix} f_1 - x_a \\ f_2 - y_a \\ f_3 - x_b \\ f_4 - y_b \end{bmatrix}^{(0)} \ ; \ J = \begin{bmatrix} \frac{\partial f_1}{\partial X} & \frac{\partial f_1}{\partial Y} & \frac{\partial f_1}{\partial Z} \\ \frac{\partial f_2}{\partial X} & \frac{\partial f_2}{\partial Y} & \frac{\partial f_2}{\partial Z} \\ \frac{\partial f_3}{\partial X} & \frac{\partial f_3}{\partial Y} & \frac{\partial f_3}{\partial Z} \\ \frac{\partial f_4}{\partial X} & \frac{\partial f_4}{\partial Y} & \frac{\partial f_4}{\partial Z} \end{bmatrix}^{(0)}. \tag{25}
$$

In order to minimize $||\vec{u}||^2$, we choose [2]

$$
[\Delta X \ \Delta Y \ \Delta Z]^T = (J^T J)^{-1} J^T \vec{b}. \tag{26}
$$

Thus, the coordinate vector of the object point, suitably adjusted for measurement error, is provided by

$$
(X, Y, Z) = (X^0, Y^0, Z^0) + (\Delta X, \Delta Y, \Delta Z). \tag{27}
$$

4   Numerical Results

An experiment was conducted using a pair of fluoroscopes oriented at an angle of approximately 90° with respect to one another as this provides the maximum common field of view. In order to acquire data for the calibration of both radiographic systems, the calibration device of Figure 2 with ten control points was placed within this common field of view and a pair of stereoradiographs was thereby obtained.

For the space intersection algorithm described above, the calibration device was replaced by a test object and a second pair of stereoradiographs was so obtained. The test object consisted of a flat transparent plexiglass plate in which was embedded a two-dimensional array of radio-opaque markers each of which was 1 mm in diameter and which were separated from one another by distances ranging from 10 mm to 100 mm.

The purpose of these markers is to serve as object points in our algorithm as previously described. The three-dimensional positions of the markers relative to the laboratory coordinate system were determined *a priori* by a coordinate measuring machine (CMM). Thus, a comparison between the three-dimensional positions of these object points as measured by the CMM and their three-dimensional positions as predicted by our RSA algorithm provide a measure of the overall accuracy of the proposed procedure. In particular, the accuracy of the smoothing provided by linear orthogonal distance regression (LODR) was assessed by predicting inter-marker distances both with and without LODR.
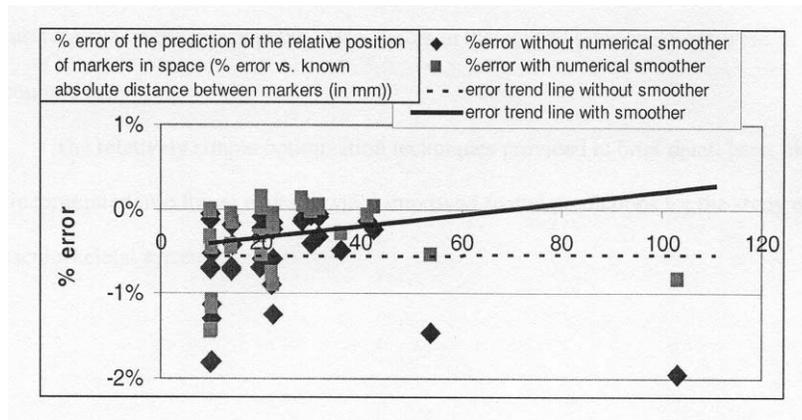
Figure 8: Error Trend Lines

Referring to Figure 8, the percentage error for each inter-marker distance both with and without LODR was plotted versus the known distance. Error trend lines fitted through these data indicate that LODR smoothing reduced the percentage error to an average of 0.3% (error range: $0.1 - 1.4\%$) as compared to an average of 0.7% (error range: $0.2 - 2.0\%$) without LODR. χ^2-errors of 1.9 with LODR and 5.47 without LODR were also computed.

5 Conclusion

The Roentgen Stereophotogrammetric Analysis (RSA) algorithm developed in the previous sections rests squarely upon the foundation laid by the pioneering work of Selvik [4] and Veress [5]. Despite being a hybrid of their techniques, our algorithm incorporates certain novel and crucial features which further reduce the degrading effects of measurement errors on this important tool of biomedical imaging.

Foremost among these innovations is the employment of linear orthogonal distance regression (LODR) [8] to minimize errors incurred while measuring the two-dimensional image locations of the fiducial (reference) markers of the calibration device. If left unchecked, these errors can result in an inaccurate computation of the projective relations between the reference and image planes and thereby degrade the accuracy of all subsequent stages of the image reconstruction process.

Our algorithm also offers improved accuracy in the determination of the locations of the perspective centers (anode positions) of the radiographic systems employed. This improvement is achieved in two ways. Firstly, during the least squares solution of the collinearity equations, image plane measurement errors are accounted for by making adjustments directly on the image plane rather than performing them on the reference plane as in previously published RSA algorithms. As shown above, this effectively removes a source of biased errors which would otherwise require variance estimations for their suppression. Secondly, we also allow for adjustments to the measured positions of the control points themselves thereby accounting for an additional source of error.

Accuracy is further enhanced by making least squares adjustments to the spatial locations of the markers implanted in the specimen. For the reasons just stated, these adjustments to the object points are performed on the image plane rather than on the reference plane. In the numerical results presented in the previous section, errors in control point locations were assumed to be equally likely in all directions so that the weighting matrix was set equal to the identity. Otherwise, estimation of coordinate error variances would be required [2].

In addition to the static validation results presented in the previous section showing that the LODR smoothing can reduce overall errors by a factor of one-half, our RSA algorithm has been shown to provide reliable tracking of low speed dynamic events [11]. Finally, our algorithm has been applied in a clinical setting to study the important problem of the ligament straining which can occur during total knee replacement surgery [12].

References

[1] R. A. Hirvonen, *Adjustment by Least Squares in Geodesy and Photogrammetry*, Ungar, New York, 1971.

[2] K. W. Wong, Basic Mathematics of Photogrammetry, in C. C. Slama (Ed.), *Manual of Photogrammetry, Fourth Edition*, pp. 37-101, American Society of Photogrammetry, Falls Church, VA, 1980.

[3] R. E. Herron, Biostereometric Measurement of Body Form, *Yearbook of Physical Anthropology* 16 (1972), 80-121.

[4] G. Selvik, Roentgen Stereophotogrammetry: A method for the study of the kinematics of the skeletal system, *Acta Orthopaedica Scandinavica Supplementum* 60(232) (1989), 1-51.

[5] S. A. Veress, X-Ray Photogrammetry, Systems, and Applications, in H. M. Karara (Ed.), *Non-Topographic Photogrammetry*, pp. 167-186, American Society for Photogrammetry and Remote Sensing, Bethesda, MD, 1989.

[6] B. Hallert, *X-ray Photogrammetry: Basic Geometry and Quality*, Elsevier, Amsterdam, 1970.

[7] W. C. Graustein, *Introduction to Higher Geometry*, Macmillan, New York, 1930.

[8] Å. Björck, *Numerical Methods for Least Squares Problems*, SIAM, Philadelphia, 1996.

[9] B. J. McCartin, A Geometric Characterization of Linear Regression, *Statistics* 37(2) (2003), 101-117.

[10] B. J. McCartin, Geometry of Linear Regression with Correlated Errors, *Statistics* 39(1) (2005), 1-11.

[11] J. Benny, B. McCartin, L. Pack, P. Morse, P. J. Atkinson, The use of Roentgenstereofluorogrammetry to predict the 3-D spatial coordinates of points in low speed events, *Journal of Biomechanics* 35(7) (2002), 1003-1006.

[12] T. Atkinson, P. Atkinson, L. Pack, J. Benny, B. McCartin, P. Morse, R. Jain, Anterior Tibial Retraction During Total Knee Arthroplasty Produces Significant Collateral Ligament Strains, *Proceedings of the ASME Summer Bioengineering Conference*, BED-Vol. 50 (2001), 391-392.